Infinitely Robust Order and Local Order-Parameter Tulips in Apollonian Networks with Quenched Disorder

C. Nadir Kaplan,[1,2] Michael Hinczewski,[3,4] and A. Nihat Berker[1,3,5]

[1]*Department of Physics, Koç University, Sarıyer 34450, Istanbul, Turkey,*
[2]*Martin Fisher School of Physics, Brandeis University, Waltham, Massachusetts 02454, U.S.A.,*
[3]*Feza Gürsey Research Institute, TÜBITAK - Bosphorus University, Çengelköy 34684, Istanbul, Turkey,*
[4]*Department of Physics, Technical University of München, 85748 Garching, Germany, and*
[5]*Department of Physics, Massachusetts Institute of Technology, Cambridge, Massachusetts 02139, U.S.A.*

For a variety of quenched random spin systems on an Apollonian network, including ferromagnetic and antiferromagnetic bond percolation and the Ising spin glass, we find the persistence of ordered phases up to infinite temperature over the entire range of disorder. We develop a renormalization-group technique that yields highly detailed information, including the exact distributions of local magnetizations and local spin-glass order parameters, which turn out to exhibit, as function of temperature, complex and distinctive tulip patterns.

Although their structure dates back to ancient Greek mathematics, Apollonian networks [1, 2] have seen a recent surge of interest as a simple and elegant model that incorporates some of the key features identified in real-world networks: a scale-free degree distribution, the small-world effect, and a high clustering coefficient. As such, they have become a versatile tool for understanding the effects of complex topologies in interacting systems: applications include percolation and epidemic spreading [1, 3], magnetic systems [1, 4], mechanisms of network growth [5], avalanches in sandpile models [6], neural networks [7], and even quantum behaviors like coherent exciton transport [8] and correlated electron models [9, 10]. The latter were inspired by the development of synthetic, nanoscale, non-branched fractal polymers [11], which raises the possibility that the unique properties of scale-free structures like Apollonian networks may be harnessed for technological applications.

In this study we focus on an intriguing aspect of these networks: their ordering resilience in the presence of imposed quenched disorder. For an Ising model with a variety of random-bond distributions – ferromagnetic/antiferromagnetic percolation and spin-glass – we find that ordered phases persist up to infinite temperature, for every case except the pure antiferromagnetic system (where the geometrical frustration of the network leads to paramagnetism). The self-similar nature of the Apollonian network allows the use of exact renormalization-group (RG) techniques to calculate the phase diagram structure, even in the presence of quenched randomness. While there have been many numerical RG studies of spin glasses on fractal lattices, we have gone further, developing an iterative procedure based on the local recursion matrix that allows us to calculate exactly the complete distribution of the local magnetization and spin-glass order parameters, for the full range of bond probabilities and temperatures. The resulting local-order diagrams (Fig. 1) show an intricate structure as temperature is lowered, never before observed in such detail for a disordered spin system. Apollonian networks can be embedded in a Euclidean plane

without any edge crossings [1, 2]. This makes spin systems on such networks potentially physically realizable, for example in nanostructures formed from dense polydisperse packings of magnetic grains [1, 4].

Network structure – The construction of the Apollonian network is depicted in Fig. 2(a): at each step, a new site is added to the center of every triangle in the network, and connected to the surrounding vertices. In the limit of infinite size, the geometrical characteristics of the network can be summarized as follows [1, 2, 12]: $P(k)$ being the probability that a site has degree k, the cumulative degree distribution is $P_{\mathrm{cum}}(k) = \sum_{k'=k}^{\infty} P(k) \sim k^{1-\gamma}$ for large k, with the scale-free exponent $\gamma = 1 + \ln 3 / \ln 2 \approx 2.585$. Due to the compact network structure, the average shortest-path length $\bar{l}$ between any two points scales as in the small-world effect, $\bar{l} \sim \ln N$, as shown in [12] using the exact recursive method of [13]. As is typical in small-world networks, the average clustering coefficient is large, $C \approx 0.828$, measuring the ratio of the connections among the nearest-neighbors of a site and the maximum possible number of such connections $k(k+1)/2$, where k is the degree of the site. In all these respects the topological properties of the Apollonian network are comparable to those observed in empirical complex networks that are simultaneously scale-free and small-world [14].

We study an Ising Hamiltonian on the network, $-\beta\mathcal{H} = \sum_{\langle ij \rangle} J_{ij} s_i s_j$, where $s_i = \pm 1$, $\beta = 1/k_B T$, the sum $\langle ij \rangle$ is over nearest neighbors, and the bond strengths J_{ij} are distributed with a quenched random probability distribution $P(J_{ij})$. We consider two types of distributions described by bond probability p : (i) the percolation case, where $P(J_{ij}) = p\delta(J_{ij} - J) + (1-p)\delta(J_{ij})$, for both ferromagnetic (F) $J > 0$ and antiferromagnetic (AF) $J < 0$ interactions; (ii) the $\pm J$ spin glass (SG) case, where $P(J_{ij}) = p\delta(J_{ij} + J) + (1-p)\delta(J_{ij} - J)$ with $J > 0$.

Exact renormalization-group transformation – The self-similar structure of the Apollonian network allows us to formulate an exact RG transformation. For $-\beta\mathcal{H}(\{J_{ij}\})$ the Hamiltonian for a particular configuration of interactions on the nth-generation network (*i.e.*, the lattice after
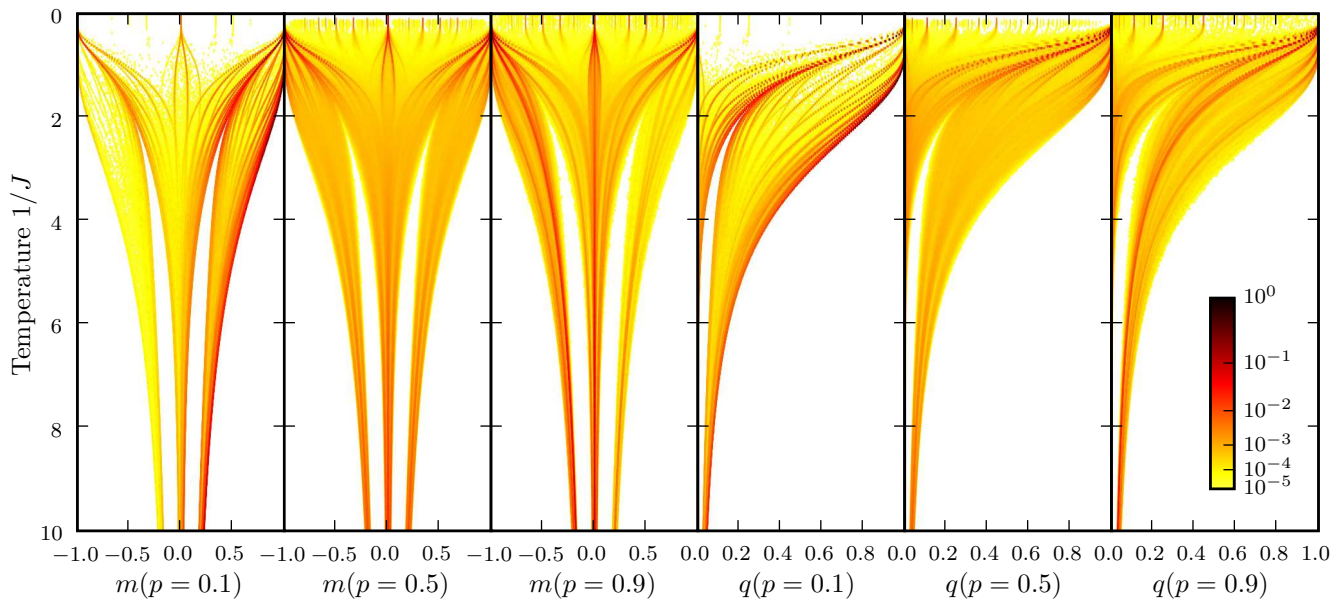
FIG. 1: Local order-parameter tulips: Probability distributions of local magnetization (left panels) and spin-glass (right panels) order parameters of the interior sites on an Apollonian network with Ising spin-glass interactions, as a function of temperature, for three different antiferromagnetic bond concentrations p.
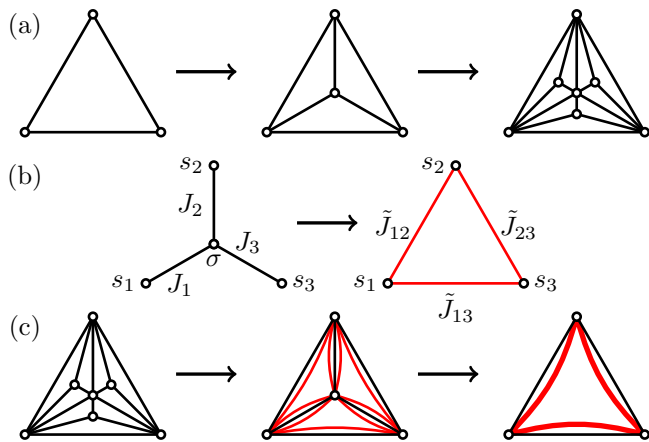

FIG. 2: (a) Construction of an Apollonian network. (b) Star-triangle transformation. (c) Two successive RG transformations of an Apollonian network.

n construction steps), the RG mapping yields a Hamiltonian $-\beta'\mathcal{H}'(\{J'_{ij}\})$ with a renormalized set of interactions $\{J'_{ij}\}$ on the $(n-1)$th-generation network, preserving the partition function. The mapping is carried out through a star-triangle transformation, tracing over the spins at sites added at the nth step. This is shown for one plaquette in Fig. 2(b), with the decimated spin labeled σ. The trace over σ produces interactions $\tilde{J}_{12}$, $\tilde{J}_{13}$, $\tilde{J}_{23}$, between the edge sites of the triangle, which are functions of the original interactions J_1, J_2, J_3 of the star. In the context of the whole network, the mapping works as shown in Fig. 2(c). The $\tilde{J}_{ij}$ interactions (inner to each triangle) are added to the original interactions J_{ij} of the

$(n-1)$th generation network (in-between triangles), to give the renormalized interactions J'_{ij}. Thus, in the bulk each original interaction gets $\tilde{J}_{ij}$ contributions from its two adjoining plaquettes.

In order to implement this RG transformation for the system in the thermodynamic limit, we focus on the probability distribution of triplets $Q(\{\tilde{J}_{ij},\ \tilde{J}_{jk},\ \tilde{J}_{ik}\})$ generated by the star-triangle transformation. As we iterate the RG mapping, this distribution Q changes, and we can extract thermodynamic information from the resulting flows. To keep track of Q at each step, we adapt a numerical procedure developed by Nobre [15] for RG transformations of spin glasses on hierarchical lattices. This method has been shown to give numerically accurate results for phase diagrams [16], agreeing with more complicated binning techniques used to directly evaluate the RG flows of interaction distributions [13]. We represent the distribution Q by a pool of large size M, where each element in the pool consists of a triplet of real numbers. To generate the initial pool $Q^{(1)}$, we repeat the following M times: (i) choose three random numbers J_1, J_2, J_3 with the probability $P(J)$; (ii) perform the star-triangle transformation of Fig. 2(b), yielding a triplet $\{\tilde{J}_{12}, \tilde{J}_{23}, \tilde{J}_{13}\}$ which is placed in the pool. Each subsequent RG transformation creates a new pool $Q^{(i)}$ from the previous pool $Q^{(i-1)}$ in the following manner, again repeating the same procedure M times to preserve the size of the pool: (i) randomly choose three triplets from $Q^{(i-1)}$; (ii) randomly arrange these three triplets like the three triangles in the second step of Fig. 2(c), together with the three middle bonds, chosen randomly with probability $P(J)$; (iii) decimate the center spin to yield a renormalized triplet, namely the inner bonds in the third step of Fig. 2(c)),
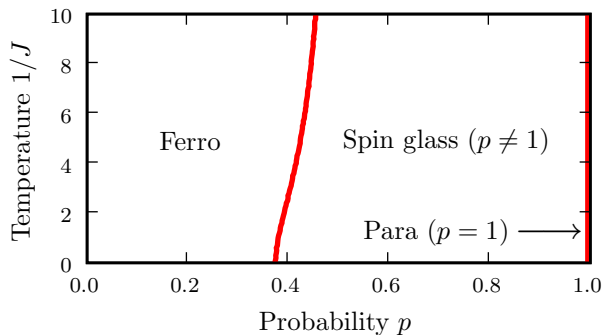
FIG. 3: Phase diagram of the Ising spin glass on an Apollonian network, in temperature $1/J$ versus antiferromagnetic bond concentration p. The boundary between the ferromagnetic and spin-glass phases is first order. The paramagnetic phase appears with a first-order phase transition at $p = 1$.

which is placed in pool $Q^{(i)}$. As $M \to \infty$, the pools mimic the exact renormalized distributions of triplets in the thermodynamic limit. For the present work, we found that $M = 10^6$ was sufficiently large to make finite-ensemble effects negligible. From the behaviors of the $Q^{(i)}$ in the limit of large i, we can identify the phase structure of the system. Specifically, looking at the average $\bar{J}^{(i)}$ and standard deviation $\sigma_J^{(i)}$ of the $3M$ bond strengths in pool $Q^{(i)}$, we can distinguish three limiting behaviors as $i \to \infty$: (i) a ferromagnetic (F) sink, where $\bar{J}^{(i)} \to \infty$, $\sigma_J^{(i)} \to \infty$, $\sigma_J^{(i)}/\bar{J}^{(i)} \to 0$; (ii) a spin-glass (SG) sink, where $\bar{J}^{(i)} \to \infty$, $\sigma_J^{(i)} \to \infty$, $\bar{J}^{(i)}/\sigma_J^{(i)} \to 0$; (iii) a paramagnetic (P) sink, where $\bar{J}^{(i)} \to 0$, $\sigma_J^{(i)} \to 0$.

Calculation of local magnetizations and local SG order parameters – Moreover, the numerical procedure described above is not limited to just the distribution of renormalized interactions Q. It can be extended to determine additional thermodynamic details, in particular the distribution of local magnetizations and local SG order parameters. Let us consider the magnetization m_σ at a site σ in the original lattice. For simplicity, let σ be one of the sites generated at the last construction step. We shall denote these as "interior sites", and they constitute 2/3 of the total lattice in the limit of large n. Adding a local magnetic field H_σ, we can write $m_\sigma = \partial \ln Z/\partial H_\sigma|_{H_\sigma=0}$, where Z is the partition function. The star-triangle transformation with H_σ produces additional interactions in the renormalized triangle on the right side of Fig. 2(b): three local fields $H_1 s_1, H_2 s_2, H_3 s_3$, and a three-site term $K s_1 s_2 s_3$, where H_i and K are functions of the J_{ij} and H_σ. With these interactions, the RG mapping is closed upon further iteration, so there will be a set of parameters $\mathbf{K}^{(i)} \equiv \{H_1^{(i)}, H_2^{(i)}, H_3^{(i)}, K^{(i)}\}$ after the ith RG step associated with the triangle that originally contained spin σ. Using the chain rule, m_σ can be expressed [17, 18] in terms of local recursion matrices T over the i steps,

$$m_\sigma = \boldsymbol{\mu}^{(i)T} T^{(i)} T^{(i-1)} \cdots T^{(2)} \mathbf{V}^{(1)}, \qquad (1)$$
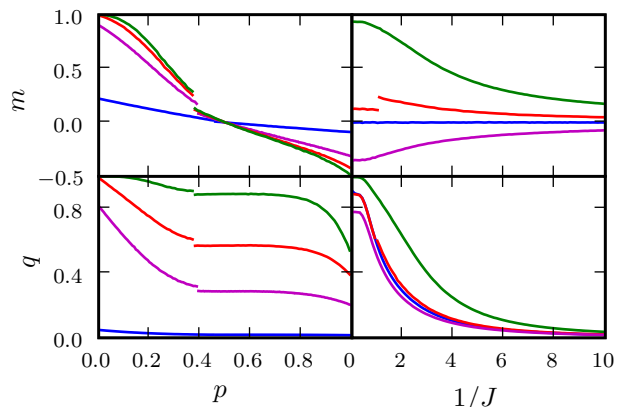

FIG. 4: Magnetization m and spin-glass order parameter q for the Ising spin glass on an Apollonian network. In the left panels, the curves, consecutively from the top, are for constant temperature $1/J = 0.2, 1.0, 2.0, 10.0$. In the right panels, the curves, consecutively from the top, are for antiferromagnetic bond concentration $p = 0.10, 0.38, 0.50, 0.90$.

where $\mu_\alpha^{(i)} = \partial \ln Z/\partial K_\alpha^{(i)}$, $T_{\beta\alpha}^{(i)} = \partial K_\beta^{(i)}/\partial K_\alpha^{(i-1)}$, $V_\alpha^{(1)} = \partial K_\alpha^{(1)}/\partial H_\sigma$, and $K_\alpha^{(i)}$ are the components of $\mathbf{K}^{(i)}$. All these quantities are evaluated in the RG subspace with initial condition $H_\sigma = 0$ (*i.e.*, where $K_\alpha^{(i)} = 0$ for all i), which makes them functions only of the J_{ij} configuration at the previous step. In the thermodynamic limit, as a corner boundary condition, we calculate $\boldsymbol{\mu}^{(i)}$ over the up-magnetized configurations of the three original corner spins of the network. As the RG transform is iterated, each triplet in the pool $Q^{(1)}$ has a corresponding vector $T^{(i)} \cdots T^{(2)} \mathbf{V}^{(1)}$, which can be contracted with $\boldsymbol{\mu}^{(i)}$ calculated from $Q^{(i)}$ to obtain a pool of m_σ using Eq. (1). For sufficiently large i and M, the resulting pool converges to the exact distribution of local magnetizations in the thermodynamic limit. The averages of m_σ and $q_\sigma \equiv m_\sigma^2$ over this distribution respectively yield the magnetization m and SG order parameter q for the interior sites.

Results – We focus first on the ferromagnetic (F) and antiferromagnetic (AF) percolation cases. For F percolation the system is ferromagnetically ordered at all finite temperatures for any $p > 0$, directly related to the existence of a giant connected component in the network at all nonzero bond probabilities [1]. In contrast, one might expect macroscopic order in the system to be inhibited in the AF case, since AF bonds are frustrated on the triangular plaquettes in the network. Indeed, in the case of $p = 1$, namely for a pure AF system, frustration leads to a paramagnetic phase at all temperatures. However, as soon as even a tiny fraction of AF bonds is removed, namely for any $0 < p < 1$, we find an SG phase *at all temperatures*, an interesting example of a glassy phase which is completely impervious to thermal excitations. The SG phase appears even when weaker forms of disorder are added to the pure AF system, such as simply attenuating a fraction of the bonds. Consider

the range of models described by the bond distribution $P(J_{ij}) = p\delta(J_{ij} - J) + (1-p)\delta(J_{ij} - cJ)$ where $J < 0$ and $0 \leq c < 1$. Here $c = 0$ corresponds to the AF percolation case described above, but it turns out that any $c < 1$ gives the same phase diagram structure: a SG phase of infinite extent for all $0 < p < 1$ and paramagnetism at $p = 1$.

We now turn to the spin-glass system: The system composed of antiferromagnetic bonds, under infinitesimal doping by ferromagnetic bonds, produces a spin-glass phase via a jump, namely a first-order phase transition at $p = 1$. For a sufficient quantity of ferromagnetic doping, a first-order transition occurs to the ferromagnetic phase, as can seen in the phase diagram in Fig. 3. On both sides of the transition line the ordered phases persist to infinite temperature $1/J$, and the boundary itself asymptotically approaches a vertical line at $p = 0.5$ as $1/J \to \infty$. The first-order nature of the ferromagnetic-spinglass phase transition, to our knowledge not seen in other systems, is evident from the magnetization and SG order parameter plotted in Fig. 4, which indeed show discontinuities crossing the boundary. (At the highest temperature depicted, $1/J = 10.0$, the discontinuities exist but are too small to be seen on the scale of the figure.) Fig. 4 also reveals a curious aspect of spin-glass order on the Apollonian network: unlike a conventional spin-glass phase, the magnetization m is generally nonzero. With the above-mentioned boundary condition on the three corner spins, $m \gtrless 0$ for $p \lessgtr 0.5$. The negative m at large p is understood from the influence of the corner spins, which except for the central spin have the highest degree in the network. In an environment with mostly antiferromagnetic bonds, an up orientation for the corner spins will yield a negative magnetization of the interior sites. This ability of the most connected spins to determine the sign of the magnetization may be a general feature of scale-free networks, and has been seen in the Barabási-Albert model [19].

The evolution of the system under disorder is obtained in microscopic detail by the calculation of the local magnetizations and local SG order parameters, as described above. The resulting full distributions of the local magnetizations and SG order parameters are given in Fig. 1. To produce these graphs, the m_σ and q_σ pools were coarse-grained using a binning procedure, and the normalized heights of the resulting histograms color-coded. For clarity, histograms smaller than 10^{-5} are not shown. The distributions exhibit a distinctive tuliplike shape, developing a rich structure as the system is cooled, spreading from narrowly localized peaks at high temperatures into complex bands of smaller peaks over the whole range at intermediate temperatures. These bands in turn converge toward the expected sharply defined values at low temperatures, with local magnetization peaked around 1, 0, and -1, and the SG order parameter around 0 and 1. The asymmetry leading to negative magnetization m for $p > 0.5$ is evident in comparing the $p = 0.5$ and $p = 0.9$ local magnetization plots. The former is entirely symmetric between negative and positive peaks, while in the latter the predominance of antiferromagnetic bonds leads to the bands of negative peaks becoming more prominent.

In conclusion, we have shown that ferromagnetic and spin-glass phases on Apollonian networks exhibit a remarkable robustness, with an infinite critical temperature for any amount of disorder. This property should have consequences for actual applications on networks. For example, interacting objects arranged on Apollonian nanostructures would be able to maintain cooperative behavior over a broad range of temperatures and intrinsic disorder. Additionally, the numerical methods developed here to calculate exact distributions of local order parameters provide a uniquely detailed window onto a spin glass on a physically realizable lattice.

[1] J.S. Andrade Jr., H.J. Herrmann, R.F.S. Andrade, and L.R. da Silva, Phys. Rev. Lett. **94**, 018702 (2005).
[2] J.P.K. Doye and C.P. Massen, Phys. Rev. E **71**, 016128 (2005).
[3] T. Zhou, G. Yan, B.-H. Wang, Phys. Rev. E **71**, 046141 (2005).
[4] R.F.S. Andrade and H.J. Herrmann, Phys. Rev. E **71**, 056131 (2005).
[5] F. Comellas, H.D. Rozenfeld, and D. ben-Avraham, Phys. Rev. E **72**, 046142 (2005).
[6] A.P. Vieira, J.S. Andrade Jr., H.J. Herrmann, and R.F.S. Andrade, Phys. Rev. E **76**, 026111 (2007).
[7] G.L. Pellegrini, L. de Arcangelis, H.J. Herrmann, and C. Perrone-Capano, Phys. Rev. E **76**, 016107 (2007).
[8] X. Xu, W. Li, and F. Liu, arXiv:0810.0824 (2008).
[9] A.M. Souza and H. Herrmann, Phys. Rev. B **75**, 054412 (2007).
[10] A.L. Cardoso, R.F.S. Andrade, and A.M.C. Souza, arXiv:0809.4087v1 (2008).
[11] G.R. Newkome, *et al.*, Science **312**, 1782 (2006).
[12] Z. Zhang, L. Chen, S. Zhou, L. Fang, J. Guan, and T. Zou, Phys. Rev. E **77**, 017102 (2008).
[13] M. Hinczewski and A.N. Berker, Phys. Rev. E **73**, 066126 (2006).
[14] R. Albert and A.-L. Barabási, Rev. Mod. Phys. **74**, 47 (2002).
[15] F. D. Nobre, Phys. Rev. E **64**, 046108 (2001).
[16] M. Ohzeki, H. Nishimori, and A.N. Berker, Phys. Rev. E **77**, 061116 (2008).
[17] S.R. McKay and A.N. Berker, Phys. Rev. B **29**, 1315 (1984).
[18] D. Yeşilleten and A.N. Berker, Phys. Rev. Lett. **78**, 1564 (1997).
[19] A. Aleksiejuk, J.A. Hołyst, and D. Stauffer, Physica A **310**, 260 (2002).